

Zr–P-modification of the γ -Al₂O₃ support of cobalt-containing catalysts for the Fischer–Tropsch synthesis

O. A. Kungurova,^{a,b,c*} N. V. Shtertser,^{a,b} E. Yu. Gerasimov,^{a,b} N. V. Dorofeeva,^{c,d} O. V. Vodyankina,^c and A. A. Khassin^{a,b}

^aNovosibirsk State University, Research and Educational Center for Energoefficient Catalysis,
2 ul. Pirogova, 630090 Novosibirsk, Russian Federation.

E-mail: olya-sky@inbox.ru

^bBoriskov Institute of Catalysis, Siberian Branch of the Russian Academy of Sciences,
5 prosp. Akad. Lavrent'eva, 630090 Novosibirsk, Russian Federation

^cTomsk State University,
36 prosp. Lenina, 634050 Tomsk, Russian Federation

^dTomsk Polytechnical University,
30 prosp. Lenina, 634050 Tomsk, Russian Federation

The cobalt-containing catalysts based on alumina modified by zirconium and phosphorus additives were synthesized for the Fischer–Tropsch synthesis. Zirconium cations and phosphate anions are adsorbed onto the surface of the support oxide phase (γ -Al₂O₃) or incorporated into cobalt-containing oxide. The modification of the support probably prevents the insertion of cobalt cations into γ -Al₂O₃ and favors the formation of larger Co–Al oxide particles with the spinel-like structure. The cobalt systems based on the unmodified support have the highest catalytic activity in the Fischer–Tropsch synthesis at 230 °C ($\sim 10 \text{ mmol}_{\text{CO}} (\text{g}_{\text{cat}} \text{ h})^{-1}$ at a CO conversion of 20–23%).

Key words: cobalt-containing catalysts, modification, zirconium, phosphorus, Fischer–Tropsch synthesis.

One of the processes used for preparation of synthetic liquid hydrocarbons from gas and defined as the gas-to-liquid (GLT) technology is based on the catalytic Fischer–Tropsch synthesis (FTS). It is known that the use of the cobalt catalysts in the FTS at low temperature gives predominantly aliphatic liquid hydrocarbons. Oxides with a highly developed specific surface and mechanical strength (SiO₂, Al₂O₃, TiO₂, ZrO₂) are used as supports for highly dispersed cobalt catalysts. Pyrophoric metallic nanosized cobalt particles formed by reduction of the surface cobalt oxo compounds are active sites in catalytic transformations. The dispersion of particles of the active component and their interaction with the support play an important role in these catalysts. Some portion of surface precursors of cobalt can react with the support during thermal treatment to decrease the fraction of reducible cobalt cations. For example, the interaction of alumina with cobalt precursors leads to the formation of spinel-like phases Co_{3–x}Al_xO₄ (0 ≤ x ≤ 2).^{1,2} Correspondingly, the formation of catalytically active sites by the reduction of cobalt cations is complicated. It occurs at higher temperatures than with individual oxide Co₃O₄, and that can affect the dispersion of metallic particles and the fraction of the metallic cobalt surface accessible to the reagents.^{1–3} The dis-

persion of particle plays the decisive role: the smaller the particle sizes, the more crystallization sites and the stronger the interaction.

The chemical interaction between the support and active component can substantially be decreased by the chemical modification of the support and a proper choice of the method of introduction of cobalt compounds into the composition. Among a large variety of elements and their compounds, Zr and P are interesting modifying additives. It is known from literature data that the introduction of small amounts of phosphate into the composition of the cobalt–aluminum catalysts results in an enhancement of the level and stability of the catalytic activity of the Fischer–Tropsch reaction compared to those of the unmodified system. This is achieved due to a more uniform distribution of highly dispersed cobalt particles having a lower onset temperature for their reduction.⁴ The influence of the introduction of precursors of zirconium oxide into the composition of the cobalt–aluminum systems on the catalytic characteristics was studied by several research groups. It was found that the introduction of zirconium into Co–Al₂O₃ prevented aggregation of cobalt particles and formation of cobalt aluminates during the reaction.⁵ The presence of zirconium oxide exerts an insignifi-

cant effect on dispersion and reducibility of the catalyst but at low pressures significantly increases the selectivity for C₅₊ (see Ref. 6). At the same time, there are data indicating that the degree of dispersion of cobalt particles increases in the presence of ZrO₂ additives on the Al₂O₃ and SiO₂ supports. It was elucidated, however, that the temperature of reduction of cobalt oxides increases and the fraction of cobalt reducible at moderate temperatures decreases.^{7,8} The cobalt-containing catalysts prepared by the combined introduction of zirconium and phosphorus with different weight ratio Zr : P were studied.⁹ Silica was used as a support. All catalysts contained 0.5 wt.% Ru. The catalyst with 9.5% Zr and 0.5% P showed the highest initial conversion of CO (99%), which decreased to 85% in 70 h, whereas the conversion on the catalyst with 9% Zr and 1% P within the same time interval decreased from 96 to 54%. The authors⁹ did not compare their data with the results obtained for the catalysts based on the unmodified support and did not discuss the interaction of the third promoter (ruthenium) with Zr and P. However, it can be expected that the Zr- and P-promoted FTS catalysts are active and selective in the synthesis and their studies are promising. No works on the influence of the combined presence of the Zr and P compounds in the cobalt—aluminum catalysts on their activity were found in the literature.

The aim of this work was to investigate the influence of the method of depositing cobalt on alumina and introduction of phosphorus and zirconium additives on the phase composition, the character of formation of particles of the active component, and the catalytic activity in the Fischer—Tropsch process.

Experimental

The γ -Al₂O₃ support (AOK-78-59, SKTB Novosibirsk, fraction 0.5–1 mm) was modified by the successive impregnation first with an aqueous solution of H₃PO₄ (special purity grade) and then with an aqueous solution of ZrO(NO₃)₂·xH₂O (Arcos) and AcOH (reagent grade). The content of P in the support was 1.85 wt.%, and that of Zr was 5.45 wt.%. When choosing the phosphorus content, we were guided by comparative physicochemical data on the Co—P(x)—Al₂O₃ (x = 0–5 wt.%) catalysts.⁴ The atomic amount of Zr chosen somewhat exceeded the amount of P ($n_{Zr} : n_P = 1.25$). In this way, zirconium excess was ensured for the case if its portion would be consumed by the formation of stoichiometric zirconium phosphates (ZrP₂O₇, Zr₃(PO₄)₄). After each step of introduction of modifying compounds, the samples were dried at 150 °C and calcined at 400 °C. The obtained support was designated as (ZrP)Al. The precursor of the active component was deposited on the γ -Al₂O₃ and (ZrP)Al supports by two methods: incipient wetness impregnation with an aqueous solution of Co(NO₃)₂·6H₂O (reagent grade, GOST 4528-78) and impregnation with a melt of salts Co(NO₃)₂·6H₂O·2NH₄NO₃. The obtained systems were designated as Co—Al(s), Co—(ZrP)Al(s), and Co—Al(m),

Co—(ZrP)Al(m), respectively. The theoretical weight content of cobalt was 14.2 wt.% in all samples. After each synthesis, all samples were treated in air for 4 h at 400 °C.

To determine the composition of the prepared catalysts, the samples were dissolved in a mixture of acids (HCl, HNO₃) and the obtained solutions were analyzed with an iCAP 6300 Duo atomic emission spectrometer with inductively coupled plasma (Thermo Scientific, USA). The X-ray phase diffraction analysis of the samples was carried out on a Shimadzu XRD-6000 diffractometer using Cu-K α radiation. IR spectra were recorded on a Thermo NIKOLET 6700 FT-IR spectrometer with an attenuated total internal reflectance (ATR) attachment in the range 4000–400 cm⁻¹ with a resolution of 4 cm⁻¹. The specific surface was determined by the method of low-temperature nitrogen adsorption on a Tristar 3100 analyzer of specific surface using the multipoint BET method. The pore volume and sizes were determined using the BJH (Barrett—Joyner—Halenda) model and the data of the adsorption and desorption isotherms obtained at the relative pressure $P/P_0 = 0.99$. The temperature-programmed reduction (TPR) was applied to identify the temperature profile characterizing the reduction of cobalt compounds on the surface of relevant materials. The TRP method was performed on a ChemiSorb 2750 chemisorption analyzer. Thermogravimetric analysis (TG) was conducted on a Netzsch STA 409 instrument. The TPR measurements were carried out under the following conditions: the sample was heated from 25 to 900 °C under the flow (20 mL min⁻¹) of the gas mixture 10 vol.% H₂/Ar with a heating rate of 10 °C min⁻¹. The TG studies of the samples were carried out in the range from 50 to 900 °C with a heating rate of 5 °C min⁻¹ in the mixture 50 vol.% H₂/Ar. Hydrogen was fed with a rate of 20 mL min⁻¹, and the protective gas (argon) was simultaneously passed through the balance with the same rate. After the catalytic experiment, the catalyst structure was studied by high-resolution transmission electron microscopy (HR-TEM) on a JEM 2010 electron microscope (JEOL, Japan) with an accelerating voltage of 200 kV and a limiting resolution for the grid of 0.14 nm. The images were detected with a charge-coupled device of the Soft Imaging System matrix (Germany). The instrument is equipped with a Phoenix energy dispersive spectrometer (EDS) of the X-ray characteristic radiation (EDAX, USA) with the semiconductor Si(Li) detector with an energy resolution of 130 eV.

The tests of the catalysts in the FTS were carried out in a tube reactor (internal diameter 14 mm, 70 mm long bed) with the stationary bed of catalyst granules at 2.1 MPa, 210 and 230 °C. The composition of the initial reaction mixture (IRM) was H₂ : CO : N₂ = 6 : 3 : 1. The catalyst granules 100–250 μ m in size were used to decrease the influence of internal diffusion. The catalyst was diluted with quartz in a volume ratio of 1 : 1, which provided isothermicity of the bed. The catalytic activity of the samples was measured at the 20–25% conversion of CO. Prior to catalytic tests, the thermal treatment and reduction of the catalyst were carried out under the conditions determined from the TG data in the reductive medium. From the DTG profile, the position of the temperature maximum in the area assigned to the formation of metallic cobalt from Co²⁺ cations which are present in binary Co—Al oxides (>350 °C) was determined. The temperature of reductive activation of the catalyst was chosen on the basis of this value (Table 1).

Table 1. Activation conditions for the catalysts and the IRM flow at temperatures of the Fischer–Tropsch reaction

Catalyst	Thermal treatment in Ar flow			Reduction in H ₂ flow			$V/NL_{IRM} (h \xi_{cat})^{-1}$	
	$T/^\circ\text{C}$	t/min	$\nu^a/^\circ\text{C min}^{-1}$	$T/^\circ\text{C}$	t/min	$\nu^a/^\circ\text{C min}^{-1}$	210 °C	230 °C
Co–Al(s)	300	30	5	560	60	2	0.81	3.31
Co–(ZrP)Al(s)	200	30	5	560	60	2	0.64	0.64
Co–Al(m)	300	30	2	530	60	2	0.99	3.47
Co–(ZrP)Al(m)	350 ^b	120	2	400	120	2	0.65	1.30

^a Heating rate.^b Thermal treatment in an air flow.

Results and Discussion

According to the elemental analysis data, the cobalt content in all studied samples is slightly lower than the expected theoretical value (Table 2).

Approximately the same decrease in the content over the theoretical value was detected for P and Zr. The difference in the theoretical and observed contents is due to the fact that only the oxides (Al₂O₃, ZrO₂, P₂O₅, Co₃O₄) were taken into account in the calculation of the theoretical content of the composition of the sample. However, as follows from the IR spectroscopic data considered below, the calcined sample of the catalyst contains hydroxyl anions as impurity and adsorbed water. The content of foreign anions is significant, and the difference between the theoretical and observed contents of Co, Zr, and P is not related to losses during preparation but is explained by the presence of the anions. It cannot be excluded that the catalyst contains adsorbed water.

The initial γ -Al₂O₃ has a well developed surface (197 m² g⁻¹) with the unimodal pore size distribution, and with the average pore diameter of 5.4 nm (see Table 2). The introduction of modifying additives led to an insignificant increase in the specific surface of the support and narrowing the curve of the pore size distribution. The average

diameter and pore volume are decreased due to the stabilization of the modifiers on the pore surface but the porous structure is essentially unaffected.

As can be seen from the texture characteristics of the calcined catalytic systems (see Table 2), the introduction of the active component by impregnation with a solution or melt results in a 31–33% decrease in the pore volume in a 18% reduction of the specific surface. For Co–(ZrP)Al(m), a value of S_{sp} decreased by 28%. The average pore diameter also decreases to 4.7 nm for the Co–Al catalysts and to 3.8 nm in the catalysts promoted by Zr and P. The difference in the values of surface area of the Co–(ZrP)Al(s) and Co–(ZrP)Al(m) samples, the average values of diameters and pore volumes of which change insignificantly, is probably explained by the measurement error.

The samples were studied by XRD phase analysis to establish the phase composition. According to the obtained data, all samples calcined at 400 °C are characterized by the presence of the well crystallized phase with the spinel structure, which is indicated by a strong diffraction maximum (Fig. 1).

According to the ICSD (Inorganic crystal structure database) data, the reflections at 38.5° and 67.2° (2 θ) indicate that the γ -Al₂O₃ phase is retained in the samples. The

Table 2. Elemental composition and texture parameters of the supports and cobalt catalysts

Composition of catalysts	Designation of catalysts	Elemental composition Co–Zr–P (wt.%)		Texture characteristics			CSR ^c /nm
		theor.	exp.	S_{sp} /m ² g ⁻¹	d_{av}^a /nm	V^b /cm ³ g ⁻¹	
γ -Al ₂ O ₃	Al	—	—	197	5.4	0.36	—
Co _x O _y /Al ₂ O ₃	Co–Al(s)	14.2–0–0	13.5–0–0	163	4.7	0.24	11
Co _x O _y /Al ₂ O ₃	Co–Al(m)	14.2–0–0	12.5–0–0	160	4.7	0.24	27
ZrO _n /PO ₄ ^{m-} /Al ₂ O ₃	(ZrP)Al	—	—	203	4.0	0.26	—
Co _x O _y /ZrO _n /PO ₄ ^{m-} /Al ₂ O ₃	Co–(ZrP)Al(s)	14.2–4.4–1.5	13.2–4.0–1.4	167	3.8	0.18	16
Co _x O _y /ZrO _n /PO ₄ ^{m-} /Al ₂ O ₃	Co–(ZrP)Al(m)	14.2–4.4–1.5	12.0–3.9–1.3	146	3.8	0.18	23

^a Average pore diameter.^b Pore volume.^c Estimation of the CSR value for the cobalt–aluminum spinel-like phases.

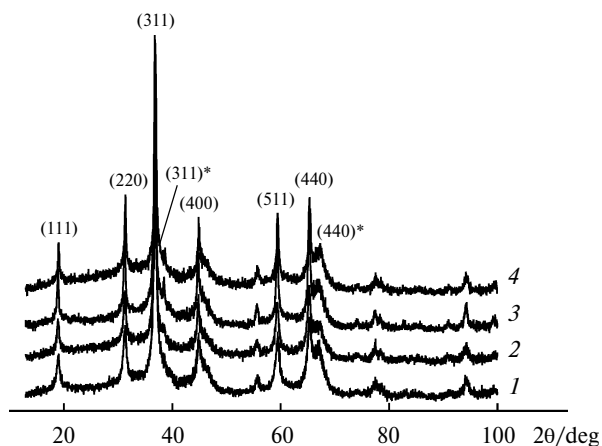


Fig. 1. Diffraction patterns of the studied catalytic materials: Co—Al(s) (1), Co—(ZrP)Al(s) (2), Co—Al(m) (3), and Co—(ZrP)Al(m) (4). Indices (hkl) and (hkl)* correspond to the diffraction lines of $\text{Co}_{3-x}\text{Al}_x\text{O}_4$ ($0 \leq x \leq 2$) and $\gamma\text{-Al}_2\text{O}_3$, respectively.

cubic cell constant determined from the reflection (440)* is 7.87 Å. The reflections with maxima at 65.2, 59.4, 44.8, 36.8, 31.2, and 18.9° are attributed to well crystallized phases with the spinel structure and composition $\text{Co}_{3-x}\text{Al}_x\text{O}_4$ ($0 \leq x \leq 2$).

The unit cell constant of the spinel structure determined from the position of the reflection from the plane [440] is 8.07 Å for the Co—Al(s) and Co—(ZrP)Al(m) samples and 8.08 Å for Co—Al(m) and Co—(ZrP)Al(s). It is known that oxides Co—Al with the spinel structure of different composition (Co_3O_4 ,^{10,11} CoAl_2O_4 , Co_2AlO_4 (see Ref. 12)) have very similar cell constants (8.07–8.10 Å). Therefore, identification and determination of the cationic composition of spinel-like phases are impossible from X-ray phase diffraction data. The sizes of coherent scattering regions (CSR) of the phases with the spinel structure in the direction [311] determined by the Debye—Scherrer equation are presented in Table 2.

The X-ray diffraction patterns of the modified catalysts exhibit no reflections characteristic of zirconia phase, which indicates either that ZrO_2 is amorphous to X-rays, or that Zr^{4+} cations interact with aluminum oxides or with Co—Al entities to form complex oxides.

The attenuated total internal reflectance IR spectra presented in Fig. 2 provide an additional information about the composition and structure of the samples.

In the range of wave numbers lower than 1000 cm^{-1} registered for samples Co—Al(s), Co—(ZrP)Al(s), and Co—Al(m), two strong absorption bands are observed at 663 and 561 cm^{-1} corresponding to vibrations of the cobalt—aluminum spinel phase. The corresponding vibrations for the crystalline phases Co_3O_4 and CoAl_2O_4 lie at 684, 563 cm^{-1} and 672, 590 cm^{-1} , respectively.¹³ The positions of these bands depend on the cationic composition of spinel and cation distribution over structural posi-

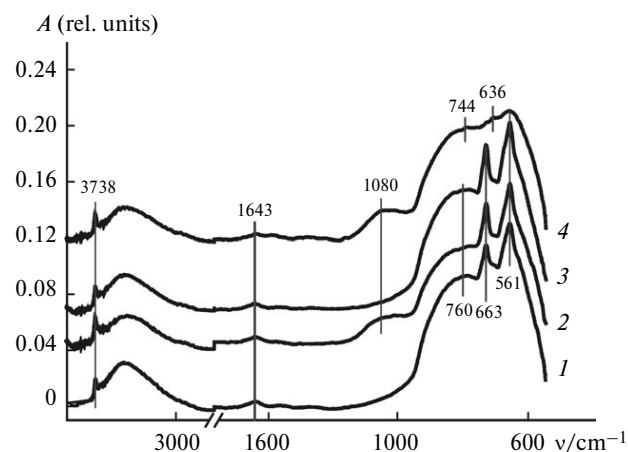


Fig. 2. IR spectra of the studied catalysts calcined at 400 °C: Co—Al(s) (1), Co—(ZrP)Al(s) (2), Co—Al(m) (3), and Co—(ZrP)Al(m) (4).

tions in the cationic sublattice. For the Co—(ZrP)Al(m) sample, the absorption bands at 630 and 564 cm^{-1} are poorly resolved and hardly visible at the background of a broad band in the range from 500 to 950 cm^{-1} , indicating a substantial violation of the order and the absence of stoichiometry in the cationic sublattice of cobalt—aluminum spinel.¹⁴

Vibrations of the $\gamma\text{-Al}_2\text{O}_3$ structure appear in the spectral range from 300 to 1100 cm^{-1} with the characteristic broad bands at 850, 650, 490, and 390 cm^{-1} (see Ref. 15). The vibrations of Al—O are presented in the spectra as a broad absorption in the range lower than 1000 cm^{-1} . Against the background of the absorption resolved lines caused by vibrations of Co—Al oxide with weakly pronounced maxima at 740–760 cm^{-1} are observed. The shift of the absorption edge and position of the maxima to lower wave numbers possibly indicate that cobalt cations enter into the oxide lattice. The shape of the IR spectra of the samples modified by Zr and P in a range of 700–1000 cm^{-1} somewhat differs from the shape of the spectra of the unmodified samples, which can be due to the interaction of the modifying additives with the $\gamma\text{-Al}_2\text{O}_3$ structure.

The IR spectra of the systems modified by phosphorus and zirconium oxo compounds (Co—(ZrP)Al(s) and Co—(ZrP)Al(m)) contain absorption bands at 1080 cm^{-1} corresponding to the P—O stretching vibrations of the PO_4^{3-} tetrahedron.^{9,16,17}

This position of the absorption band is characteristic of phosphates or phosphate anion adsorbed on the surface of the oxide phases. For aluminum phosphate, the P—O vibrations of the PO_4^{3-} tetrahedron appear in the range from 1050 to 1112 cm^{-1} , depending on the prehistory and structure of phosphate,¹⁸ and at 1118 cm^{-1} (see Ref. 9). Zirconium orthophosphate is characterized by the band at 1074 cm^{-1} (see Ref. 19).

The spectra of all samples exhibit a strong and narrow band at 3738 cm⁻¹ characteristic of vibrations of the hydroxyl groups in γ -Al₂O₃. The surface area of the peak of these vibrations is 16–17% larger for Co–(ZrP)Al(s) and Co–(ZrP)Al(m) than those for the unmodified samples. It is known that the interaction of metal cations with γ -Al₂O₃ results in a noticeable decrease in the concentration of OH groups in the oxide due to the substitution of the protons of the hydroxyl groups by the cation (see, *e.g.*, data on the Cu²⁺/ γ -Al₂O₃ system²⁰). It can be assumed that, in our case, the modification of the support prevents the interaction of cations Coⁿ⁺ with the support *via* the mechanism of substitution of the protons of the surface hydroxyl groups.

The modified samples exhibit some increase in the absorption intensity in a range of 3670 cm⁻¹, which should be assigned to vibrations of the OH groups bound to the Zr cations.²¹

The broad absorption band with a maximum in a range of 3500–3450 cm⁻¹ corresponds to symmetric stretching vibrations of OH in molecules of adsorbed/bound water. The band at 1643 cm⁻¹ corresponds to bending O–H vibrations of adsorbed water.

The results of X-ray diffraction analysis and IR spectroscopy suggest that the modification of γ -Al₂O₃ by zirconium and phosphorus cations slightly changed the phase composition of the samples obtained by depositing cobalt from a solution or a melt of cobalt nitrate. A well crystallized spinel-like phase with the CSR size more than 10 nm was formed in the samples during calcination. The use of a melt of salts for impregnation results in the formation of better crystallized particles of Co–Al oxide with the spinel structure.

Modifying zirconium cations and phosphate anions are adsorbed on the surface of the oxide phases of the support (γ -Al₂O₃) or incorporate in a cobalt-containing oxide. Probably, the modification of the support prevents the interaction of Coⁿ⁺ cations with the support, resulting in the substitution of the protons of the surface hydroxyl groups by cations. This does not exclude the formation of complex Co–Al oxides, including those with the spinel-like structure, on the areas of the alumina surface free of modifiers.

The evolution of the catalyst structure in the course of reductive activation was studied by the TPR method in a mixture of 10% H₂ in Ar (at a heating rate of 10 °C min⁻¹) and the TG method in a mixture of 50% H₂ in Ar (at a heating rate of 5 °C min⁻¹). According to the TPR and TG data, in all systems reduction of cobalt compounds to the metal proceeds in several steps (Fig. 3).

The DTG curve exhibit a low-temperature effect in the range lower than 200 °C corresponding to the removal of adsorbed water and CO₂. The hydrogen absorption and weight loss in a range of 200–400 °C are related to the reduction of the Co³⁺ cations incorporated in cobalt-con-

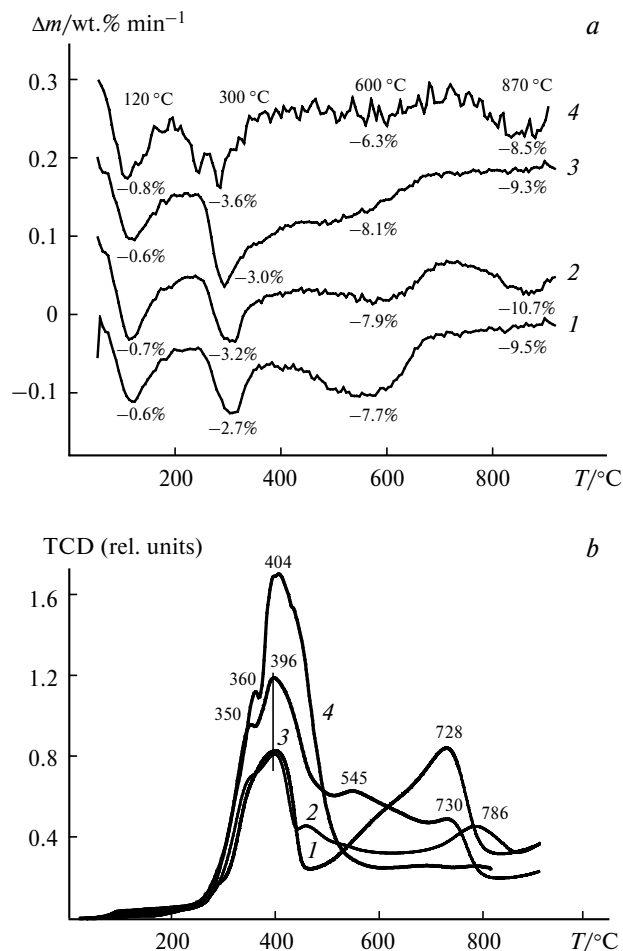


Fig. 3. DTG profiles (a) and TPR profiles (b) of the samples: Co–Al(s) (1), Co–(ZrP)Al(s) (2), Co–Al(m) (3), and Co–(ZrP)Al(m) (4). TCD is the signal from the thermal conductivity detector.

taining oxides to Co²⁺. The shoulder at 350–360 °C observed in all TPR curves is possibly due to reduction of the CoO phase formed by reduction of pure oxide Co₃O₄. The reduction of individual oxide Co₃O₄ to metallic Co⁰ is completed at temperatures not higher than 450 °C.^{1,2} Therefore, all processes that occur at higher temperatures should be assigned to the reduction of cations Co²⁺ in complex Co–Al oxides to metallic cobalt. The complex oxides can also be modified by cations Zrⁿ⁺.

Weight loss of the sample (designated by digits near the DTG curve) attains 9–11% during the reduction. The theoretical value of the weight loss observed on reduction of oxide Co₃O₄ is 0.36 of the total cobalt content, *i.e.*, not more than 4.5–5% of the sample weight. The balance of 5–6% should be attributed to the removal of impurity anions (first of all, hydroxyl groups) during the reduction.

The effects of hydrogen uptake in the TPR curves and weight losses in the DTG curves in the range higher than 450 °C differ significantly in shape and position, since the

Table 3. Catalytic parameters of the cobalt catalysts in the Fischer–Tropsch reaction at 210 and 230 °C, pressure 2.1 MPa, and synthesis-gas composition H₂ : CO : N₂ = 6 : 3 : 1

Catalyst	<i>T</i> /°C	<i>X</i> _{CO} (%)	<i>W</i> _{CO} /mmol (g _{cat} · h) ⁻¹	<i>S</i> (CH ₄) (%)	<i>S</i> (C ₅₊) (%)	C ₃ (=/-)	α _{ASF} ^a
Co—Al(s)	210	25	2.7	10	77	2.30	0.80 (12–22)
Co—(PZr)Al(s)	210	7.5	0.64	15	66	1.31	—
Co—Al(m)	210	21	2.8	11	75	2.20	0.84 (12–22)
Co—(PZr)Al(m)	210	14	1.3	12	75	0.93	—
Co—Al(s)	230	23	10.4	13	73	1.86	0.86 (9–24)
Co—(PZr)Al(s)	230	25	2.1	20	60	0.57	0.71 (16–19)
Co—Al(m)	230	20	9.5	13	73	1.95	0.84 (12–25)
Co—(PZr)Al(m)	230	26	4.4	16	69	0.79	0.84 (21–25)

^a The Anderson–Schulz–Flory (ASF) distribution parameter was determined for the products of the alkane series. The range of the number of carbon atoms in the products that were used for the determination of the parameter is indicated in parentheses. The activity of the modified catalysts at 210 °C turned out to be insufficient for the accumulation of the amount of liquid hydrocarbons necessary for analysis.

reduction conditions were different: more diluted hydrogen (10%) was used in the TPR experiments and, hence, the reduction occurred more slowly or at higher temperatures.

The catalysts of series "s" obtained by impregnation with solution are characterized by intensive effects in the high-temperature range in the TPR and DTG curves, indicating the strong interaction of cobalt with alumina. The DTG curves of the samples obtained by the impregnation of unmodified γ-Al₂O₃ exhibit peaks in a range of 500–650 °C, which is well consistent with the *in situ* X-ray diffraction data on the reduction of cobalt from complex Co—Al oxides characterized by the simple cubic cell (structure of the NaCl type).^{*} This phase is formed by the reduction of cations Co³⁺ to Co²⁺ in defect spinel-like Co—Al oxides with a high cobalt content.

The position of the high-temperature effect in the DTG curve (850–950 °C) corresponds to the reduction of cations Co²⁺ occupying tetrahedral positions of stoichiometric cobalt aluminate CoAl₂O₄. The presence of this effect in the thermal curves does not mean that the phase of stoichiometric cobalt aluminate was incorporated in the initial samples of series "s." Alternatively it could be formed from non-stoichiometric Co—Al oxide with the spinel structure during the reduction of some Co cations at 450–650 °C. During the temperature-programmed reduction in dilute hydrogen (TPR curves), this transforma-

tion is outside of the studied temperature range, and only an end part of the effect of hydrogen uptake can be observed in the curves in the range above 850 °C.

The modified samples contain the maximum amount of cobalt reduced at 850–900 °C. Therefore, it can be expected that the content of active cobalt in the modified samples reduced in the temperature range below 550 °C is lower than that in similar unmodified samples of the Co—Al catalysts.

The data obtained on the kinetics of cobalt reduction were used for choosing the reductive activation conditions prior to tests in the FTS (see Table 1). For the Co—(ZrP)Al(m) catalyst, the reduction effect in the temperature range 450–600 °C is low and, hence, this sample was reduced at 400 °C.

The data of the catalytic experiment for the reduced catalysts are presented in Table 3.

In the synthesis at 210 °C, the unmodified catalysts convert CO with almost equal rates (*W*_{CO} = = 2.7 mmol_{CO} (g_{cat} h)⁻¹ at the selectivity for C₅₊ 75–77%). The activity of the modified systems turned out to be considerably lower, and limitations to the minimum flow rate of the reaction mixture in our system did not allow measurements at 20% conversion. Therefore, the reaction rate on the Co—(PZr)Al(s) catalyst was determined at a lower conversion of CO (7.5%), and *W*_{CO} was 0.64 mmol_{CO} (g_{cat} h)⁻¹.

An increase in the reaction temperature by 20 °C resulted in an almost fivefold increase in the activity for the Co—Al catalysts, and the selectivity for C₅₊ decreased to 73%. The activity of the modified samples increased

* The results of the studies are presented in the article prepared by A. A. Khassin, I. I. Simentsova, A. N. Shmakov, N. V. Shtertser, S. V. Cherepanova, O. A. Bulavchenko, and T. M. Yur'eva.

3–3.5 times, and a 25% increase in selectivity for methane was observed. The activation energy was calculated to be ~ 120 – 135 kJ mol⁻¹. Such a high value is well consistent with the earlier published data and indicates a slight influence of diffusional retardations on the synthesis in our experiments.²²

The selectivity for high-molecular-weight hydrocarbons and the fraction of olefins in the products for the modified catalysts are also lower than those for the Co–Al catalysts, whereas the selectivity for methane is correspondingly higher.

The catalyst samples used in catalytic tests were examined by transmission electron microscopy. According to the HR-TEM data, the support represents plate-like disordered crystallites of γ -Al₂O₃ (5–10 nm) composing the agglomerates of particles with a broad size range (Fig. 4).

The systems based on the unmodified support, Co–Al(s) and Co–Al(m), have large metallic cobalt particles with the size from 15 to more than 100 nm covered with an oxide layer that could also be formed due to oxidation with air after the reaction. These particles are nonuniformly distributed over the support surface. The modified catalysts

have particles with the size to 100 nm for Co–(ZrP)Al(s) and to 500 nm for Co–(ZrP)Al(m). Many particles 15–25 nm in size are grouped into large agglomerates (see Fig. 4). Particles of metallic cobalt have a defect structure consisting of alternating domains of face centered cubic (fcc) and hexagonal primitive (hp) structures with the interplanar distance $d = 0.19$ – 0.20 nm (see Fig. 4, *a, b*).^{23,24}

The results of studies on an EDS make it possible to estimate the local elemental composition of the catalysts. Unfortunately, the energies $L_{\alpha}(\text{Zr}) = 2.042$ eV and $K_{\alpha}(\text{P}) = 2.013$ eV do not allow us to separate the contribution of X-ray radiation emission between these elements. However, the content of Zr could be detected also by the line $K_{\alpha}(\text{Zr}) = 15.744$ eV. The correlation of the integral intensity of the signals ($L_{\alpha}(\text{Zr}) + K_{\alpha}(\text{P})$) at 2.03 eV and $K_{\alpha}(\text{Zr})$ at 15.74 eV is presented in Fig. 5.

Significant nonuniform distribution of modifying elements introduced in catalysts is noteworthy: in some regions the zirconium content is 8–10%, and in other regions it is less than 2%. In the areas of the samples, where the Co : Al ratio is higher than 1, *i.e.*, in the region of localization of the cobalt-containing phases (cobalt oxide

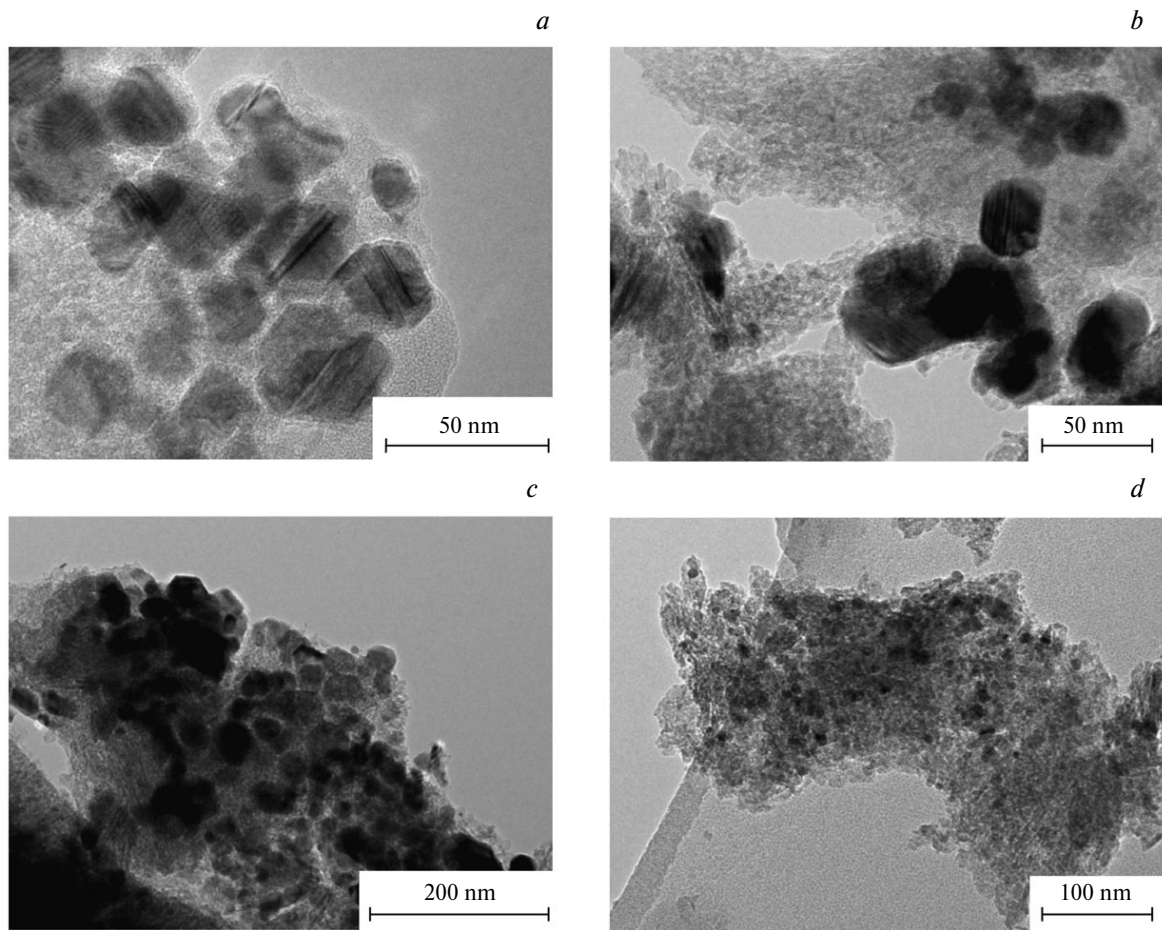


Fig. 4. HR-TEM images of the catalysts Co–Al(s) (*a*), Co–(ZrP)Al(s) (*b*), Co–Al(m) (*c*), and Co–(ZrP)Al(m) (*d*) after catalytic tests in the Fischer–Tropsch synthesis.

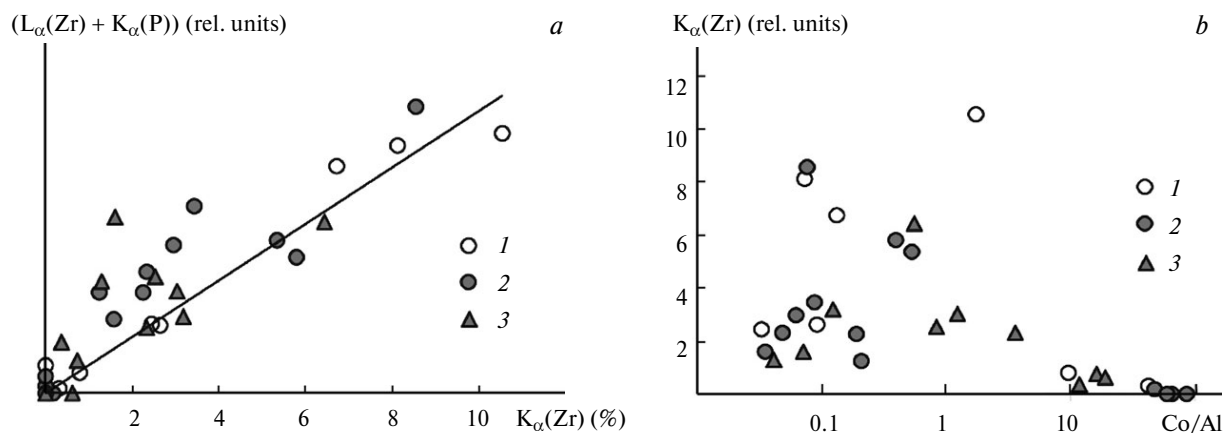


Fig. 5. Correlations of the experimental intensities of the lines obtained on the EDS at 2.03 and 15.74 eV (a) and estimates of the Zr content vs atomic ratio Co : Al (b) for the calcined sample Co—(ZrP)Al(m) (1) and samples Co—(ZrP)Al(m) (2) and Co—(ZrP)Al(s) (3) after catalytic tests.

in the oxide sample), the zirconium content decreases with an increase in the Co : Al ratio. This allows one to conclude that zirconium is predominantly bound to the support and does not form combined Co—Zr oxide phases.

The phosphorus content in the sample prepared by impregnation with melt correlates satisfactorily with the content of zirconium. This is especially pronounced in the oxide sample before reduction. Criterion R^2 for the correspondence of the dependence of the signal intensity $(L_{\alpha}(\text{Zr}) + K_{\alpha}(\text{P}))$ at 2.03 eV on $K_{\alpha}(\text{Zr})$ at 15.74 eV to the direct proportionality in the oxide catalyst Co—(ZrP)Al(m) is equal to 0.95 and decreases to 0.78 after catalytic tests. No correlation is observed in the Co—(ZrP)Al(s) catalyst: the similar value of R^2 is equal to 0.30.

According to the data of EDS measurements, the maximum content of zirconium is observed in the regions with the ratio Co : Al from 1 : 10 to 2 : 1. In the case of predomination of the support phase in the range of analysis, their content was lower than the averaged value for the sample (group of data with Co : Al from 1/30 to 1/5 and Zr content from 1 to 4%), whereas modifying elements were almost absent from the bulky cobalt particles. This possibly indicates that in the catalyst zirconium is concentrated at the metal—support interface and also decorates dispersed particles of metallic cobalt.

This assumption is confirmed by the conclusions obtained by HR-TEM. Indeed, the composition and structure of the oxide layer covering metal particles in the modified samples differ from those of pure cobalt oxide. The HR-TEM data on metal particles of the modified sample prepared by impregnation with solution are shown in Fig. 6.

The fast Fourier transform of the central region of the TEM image shows the observed interplanar spacings and interplane angles. The Fourier images corresponding to interplanar distances of 2.086 Å [100] and 1.896 Å [111] nm should be assigned to the fcc structure of metallic

cobalt (JCPDS PDF # 15-806). The angle between the planes (111) and (100) is 54.7°. Distances of 2.251 and 2.509 Å with the angle between them equal to 55.8° are observed in addition to these reflections. These images completely coincide with those expected from oxide ZrO_2 (JCPDS PDF # 37-1484): the interplanar distances are 2.25 Å [201] and 2.5 Å [001] and the angle between these planes is 55.8°. However, the Fourier-filtered image distinctly shows that the surface layer has regions close to the rhombic image with somewhat different interplanar distances. Perhaps, the composition of the oxide layer is non-uniform: one should take into account the probability of formation of regions of the CoO layer (JCPDS PDF # 42-1300) with distances between the planes of 2.62 Å (111) and 2.27 Å (100) and an angle of 54.7°, which completely coincides with the geometry of metallic Co and a fairly weak signal observed in the EDS spectra (~2 at.%). It is also admissible that the ordering effect in the form of rhombic pictures and a slight change in the interplanar distance is caused by the formation of the mixed oxide layer $\text{Co}_x\text{Zr}_y\text{O}$ on the surface of a metallic particle.

On the basis of a set of interplanar distances, we may assume that the faceted particles 1–2 nm in size observed around the metal particle in the image are assigned to the ZrO_2 phase.

Thus, the modification of the $\gamma\text{-Al}_2\text{O}_3$ support by phosphorus and zirconium compounds did not result in a significant difference in phase composition of the samples obtained by depositing cobalt from solution or melt of cobalt nitrate. After the temperature treatment in air at 400 °C, a well crystallized spinel-like phase was formed in the samples. The particle sizes of the phase range from 10 to 100 nm for the unmodified samples, and the sizes attained 100 nm for Co—(ZrP)Al(s) and 500 nm for Co—(ZrP)Al(m). The smaller content of aluminum in the cobalt-containing oxide is observed for the catalysts obtained by impregnation with melt.

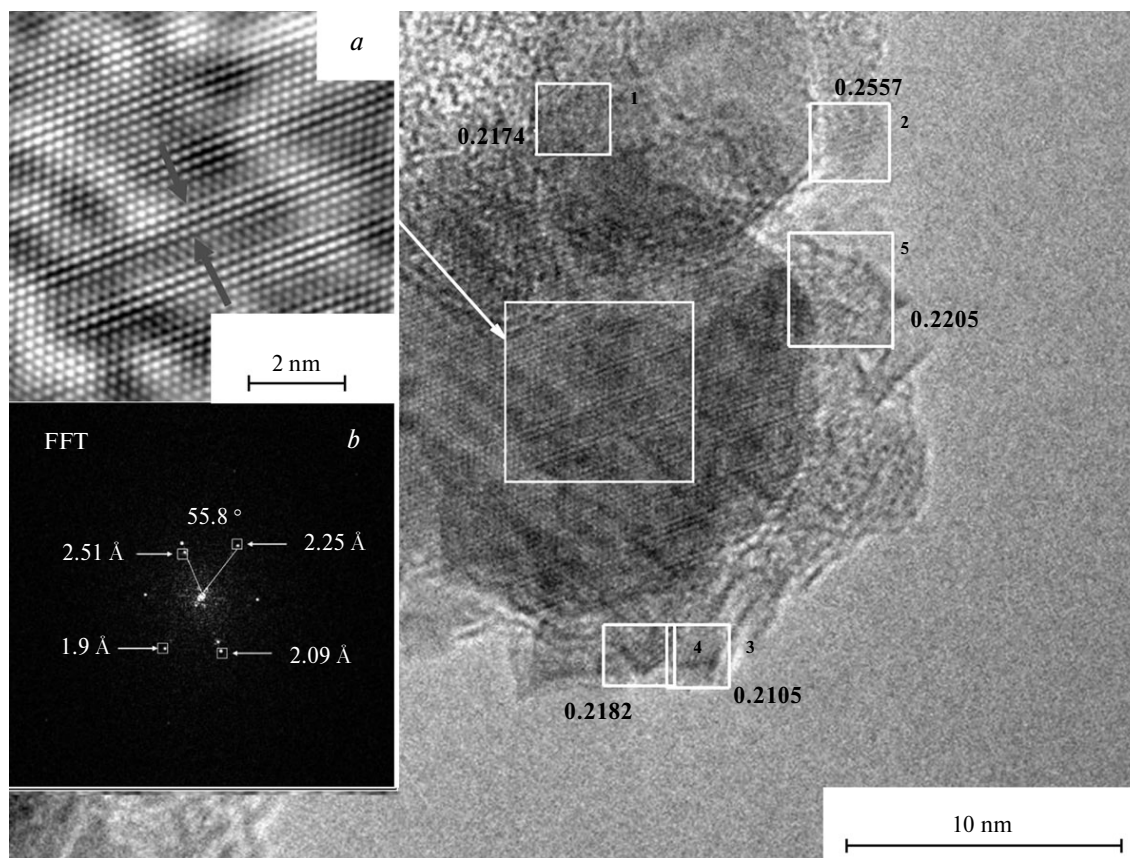


Fig. 6. HR-TEM image of the region of the Co–(ZrP)Al(s) sample after catalytic tests in the Fischer–Tropsch synthesis. Insets: (a) result of the Fourier filtration of the image of the isolated region of a metal particle showing the presence of superstructural ordering (designated by arrows); (b) set of reflections observed in this region obtained by the fast Fourier transform method.

Modifying zirconium cations and phosphate anions are adsorbed on the surface of the oxide phases of the support (γ -Al₂O₃) or incorporated into cobalt-containing oxide. The modification of the support and introduction of cobalt nitrate by impregnation with melt prevent the interaction of Coⁿ⁺ cations with the support, which proceeds *via* the substitution of the protons of the surface hydroxyl groups by cobalt cations. However, the fraction of poorly reducible cobalt increases in this case.

The size of the CSR of the Co-containing precursor oxide in the modified samples is significantly larger than that in similar samples prepared using the unmodified support. After catalytic tests of the samples containing modifying elements, zirconium oxide is converted into the reduced state and is located at the metal–support interface or decorates small particles of metallic cobalt.

The catalytic tests performed suggest a lower activity of the modified samples and the shift of their selectivity to the formation of lighter and more saturated hydrocarbons. A broader size distribution of the Co particles and the presence of large agglomerates with sizes smaller than 100–500 nm can explain a low catalytic activity of these catalysts in the Fischer–Tropsch synthesis compared to

the unmodified samples. The activity of the modified catalysts can additionally be decreased by the decoration of the surface of metallic particles by crystallized compounds of modifying elements, including zirconia.

The work was carried out at the Joint Research and Educational Center for Energoefficient Catalysis of the Novosibirsk State University and the G. K. Boreskov Institute of Catalysis, Siberian Branch of the Russian Academy of Sciences.

This work was financially supported in part by the program "Scientific Foundation named after D. I. Mendeleev at the Tomsk State University" for 2014–2015.

References

1. P. Arnoldy, J. A. Moulijn, *J. Catal.*, 1985, **93**, 38.
2. O. H. Hansteen, H. Fjellvag, B. C. Hauback, *Acta Chem. Scand.*, 1998, **52**, 1285.
3. O. A. Bulavchenko, S. V. Cherepanova, V. V. Malakhov, L. S. Dovlitova, A. V. Ishchenko, S. V. Tsybulya, *Kinet. Catal. (Engl. Transl.)*, 2009, **50**, 192 [*Kinet. Catal.*, 2009, **50**, 205].
4. J. W. Bae, S. M. Kim, Y. J. Lee, M. J. Lee, K. W. Jun, *Catal. Commun.*, 2009, **10**, 1358.

5. H. Xiong, Y. Zhang, K. Liew, J. Li, *J. Mol. Catal. A: Chem.*, 2005, **231**, 145.
6. F. Rohr, O. A. Lindveg, A. Holmen, E. A. Blekkan, *Catal. Today*, 2000, **58**, 247.
7. G. Jacobs, T. K. Das, Y. Zhang, J. Li, G. Racoillet, B. H. Davis, *Appl. Catal. A: General*, 2002, **233**, 263.
8. A. Michalak, M. Nowosielska, W. K. Jozwiak, *Top. Catal.*, 2009, **52**, 1044.
9. J. W. Bae, S. M. Kim, S. J. Park, Y. J. Lee, K. S. Ha, K. W. Jun, *Catal. Commun.*, 2010, **11**, 834.
10. W. L. Smith, A. D. Hobson, *Acta Crystallogr., Sect. B*, 1973, **29**, 362.
11. W. L. Roth, *J. Phys. Chem. Solids*, 1964, **25**, 1.
12. S. Kurajica, J. Popovic, E. Tkalcec, B. Grzeta, V. Mandic, *Mater. Chem. Physics*, 2012, **135**, 587.
13. J. Preudhomme, P. Tare, *Spectrochem. Acta, Part A*, 1971, **27**, 1834.
14. S. Hafner, F. Laves, *Z. Kristallogr.*, 1961, **115**, 321.
15. J. M. Saniger, *Mater. Lett.*, 1995, **22**, 109.
16. J. W. Bae, S. M. Kim, S. H. Kang, K. V. R. Chary, Y. J. Lee, H. J. Kim, K. W. Jun, *J. Mol. Catal. A: Chemical*, 2009, **311**, 7.
17. X. Tian, W. He, J. Cui, X. Zhang, W. Zhou, S. Yan, X. Sun, X. Han, S. Han, Y. Yue, *J. Coll. Interf. Sci.*, 2010, **343**, 344.
18. T. Roncal-Herrero, J. D. Rodriguez-Blanco, L. G. Benning, E. H. Oelkers, *Cryst. Growth Design*, 2009, **9**, 5197.
19. A. I. Orlova, S. G. Samoylov, G. N. Kazantsev, V. Yu. Volguytov, D. M. Bykov, A. V. Golubev, E. Yu. Borovikova, *Crystallogr. Repts. (Engl. Transl.)*, 2009, **54**, 431 [*Kristallografiya*, 2009, **54**, 464].
20. E. Garbowski, M. Primet, *J. Chem. Soc. Chem. Commun.*, 1991, **1**, 11.
21. L. M. Kustov, V. B. Kazansky, F. Figueras, D. Tichit, *J. Catal.*, 1994, **150**, 143.
22. M. F. M. Post, A. C. van 't Hoog, J. K. Minderhoud, S. T. Sie, *AIChE J.*, 1989, **35**, 1107.
23. L. M. Plyasova, *Rentgenografiya katalizatorov v kontroliruyemykh usloviyakh temperatury i sredy [X-ray Diffraction of Catalysts in Controlled Temperature and Medium Conditions]*, Institute of Catalysis, Siberian Branch, Russian Academy of Sciences, Novosibirsk, 2011, 184 pp. (in Russian).
24. A. Taylor, R. W. Floyd, *Acta Crystallogr.*, 1950, **3**, 285.

*Received December 5, 2014;
in revised form February 5, 2015*